The Astrophysical Journal, 658: L21–L24, 2007 March 20

CONSTRAINTS ON ACCRETION IN ULTRALUMINOUS X-RAY SOURCES FROM *SPITZER* IRS OBSERVATIONS OF NGC 4485/4490: INFRARED DIAGNOSTIC DIAGRAMS

Gerardo A. Vázquez
Physics and Astronomy Department, Johns Hopkins University, Baltimore, MD 21218; vazquez@pha.jhu.edu
Ann E. Hornschemeier
NASA/GSFC, Code 662, Laboratory for X-ray Astrophysics, Greenbelt, MD 20771; annh@milkyway.gsfc.nasa.gov
Edward Colbert
Physics and Astronomy Department, Johns Hopkins University, Baltimore, MD 21218; colbert@jhu.edu
Timothy P. Roberts and Martin J. Ward
Department of Physics, Durham University, South Road, Durham DH1 3LE, UK; t.p.roberts@durham.ac.uk, m.ward@durham.ac.uk
and
Sangeeta Malhotra
Department of Physics and Astronomy, Arizona State University, Tempe, AZ 85287-1504; sangeeta.malhotra@asu.edu
Received 2006 December 20; accepted 2007 February 1; published 2007 February 28

ABSTRACT

Constraining the astrophysical nature of ultraluminous X-ray (ULX) sources, which have X-ray luminosities exceeding 10^{39} ergs s^{-1}, has been elusive due to the optical faintness of any counterparts. With high spectral resolution observations in the ~10–30 μm wavelength range we have conducted an experiment to study six ULX sources in the NGC 4485/4490 galaxy pair. We have found that five of the six ULXs, based on mid-infrared spectral diagnostics, show the characteristic higher ionization features that are found in AGNs. The sixth source, ULX-1, is consistent with being a supernova remnant. The chief infrared spectral diagnostics used are the ratios of [S iii]/[Si ii] versus [Ne iii]/[Ne ii]. In two instances fits to the continuum and polycyclic aromatic hydrocarbon (PAH) features also indicate higher dust temperatures, which are characteristic of accreting sources. Overall, however, we find that the continuum is dominated by stellar processes, and the best diagnostic features are the emission lines. High spectral resolution studies in the mid-infrared thus appear to show great promise for determining the astrophysical nature of ULXs.

Subject headings: galaxies: general — galaxies: individual (NGC 4485, NGC 4490)

Online material: color figures

1. INTRODUCTION

Ultraluminous X-ray sources (ULXs) are generally defined as extranuclear galactic X-ray sources with X-ray luminosities $L_X \geq 10^{39}$ ergs s^{-1}, a luminosity that is seldom reached by any Galactic (Milky Way) X-ray binary (XRB). If ULXs emit their X-rays isotropically, by Eddington arguments, the central object could be a black hole (BH) with mass $M \geq 5\ M_\odot$, and for Eddington ratios of $\sim 10^{-2}$ to 10^{-1}, the implied mass of the central object is ~50–500 $M_\odot$. Therefore, some ULXs could be accreting intermediate-mass black holes (IMBHs; Colbert & Mushotzky 1999; Ptak & Griffiths 1999; Miller & Colbert 2004). The majority of ULXs, however, are likely accreting *stellar* mass black holes (e.g., ~1–10 $M_\odot$), as there appears to be a strong association between ULX sources and star formation in galaxies (Zezas & Fabbiano 2002). One popular model claims that ULXs are merely stellar mass BHs in high-mass XRBs, and mild beaming of their X-ray luminosities produces the observational illusion of extremely high X-ray luminosities (e.g., King et al. 2001; King 2006). Hundreds of ULXs are known at present (e.g., Roberts & Warwick 2000, Colbert & Ptak 2002; and *Chandra* ULX catalogs by Ptak et al.[1], Swartz et al. 2004, and Liu & Bregman 2005).

Accreting binaries such as these could be precursors to eventual gravitational radiation events. Furthermore, ULXs are important because they often dominate the total observed X-ray flux in starburst galaxies (see Colbert et al. 2004). Their connection to star formation also appears to extend to cosmologically interesting ($z \gtrsim 0.1$) look-back times (Hornschemeier et al. 2004; Lehmer et al. 2006) and may provide a cosmological tool.

Unfortunately, all but the very brightest ULX sources are too faint for detailed X-ray spectroscopy studies (the best cases must rely on the resolving power of $R = 60$ at 6.4 keV available with X-ray CCDs; Miller et al. 2004).

There is perhaps hope for ascertaining the nature of ULX sources by studying their interactions with their surroundings, such as gas, dust, and stars; such information may be captured using infrared spectral diagnostics. Genzel et al. (1998) were the first to show that ionization-sensitive indices based on mid-infrared ratios were helpful for identifying the nature of heavily obscured nuclear sources (Genzel et al. 1998; Laurent et al. 2000; Sturm et al. 2002; Peeters et al. 2004). We have thus taken advantage of the resolving power ($R \sim 600$) of the Infrared Spectrograph (IRS) on board the *Spitzer Space Telescope* to calculate highly accurate ionization diagnostic ratios.

The nearby galaxy pair NGC 4485/4490 provides an excellent opportunity for studying ULX sources (see Roberts et al. 2002). There are six ULXs in NGC 4485/4490 ($D = 7.8$ Mpc; Tully 1988, p. 221), far more than is typical (≤ 2 in most cases, and 0.2 on average; Colbert & Ptak 2002; Ptak & Colbert 2004). The unprecedented sensitivity and angular resolution afforded by the *Spitzer* IRS, coupled with the proximity of NGC 4485/4490, allow us to carry out this important experiment.

[1] Available at http://www.xassist.org.

TABLE 1

List of ULXs of the NGC 4485/4490 System Taken from Roberts et al. (2002)

ULX	R.A. (J2000)	Decl. (J2000)	Notes	L_X[a] (10^{39} ergs s^{-1})	T_{dust} (K)	τ[b] (10^{-10})	$\tau_{9.7}$ (10^{-3})
1 ……	12 30 29.5	+41 39 27	NGC 4490 radio source, possible SNR	1.0 (4.9)	50, 75, 200, 300	72000, 13000, 0.1, 1.1	3310
2 ……	12 30 30.6	+41 41 42	NGC 4485 X-1	4.0 (4.6)	135, 200	56, 2.3	4810
3 ……	12 30 30.8	+41 39 11	NGC 4490 transient X-ray source	2.9 (4.6)	90, 110	740, 240	3.93
4 ……	12 30 32.3	+41 39 18	NGC 4490 X-1	1.9 (2.6)	75, 90	2500, 960	1.75
5 ……	12 30 36.3	+41 38 37	NGC 4490 X-2	1.9 (2.6)	75, 90	8800, 16	7.94
6 ……	12 30 43.2	+41 38 18	NGC 4490 X-4	3.1 (4.4)	75, 90, 110, 135	360, 580, 190, 10	2990

Note.—Units of right ascension are hours, minutes, and seconds, and units of declination are degrees, arcminutes, and arcseconds.

[a] Numbers in parenthesis give the intrinsic (unabsorbed) luminosity.

[b] The total extinction as a function of the extinction at 9.7 μm ($\tau_{9.7}$). The total extinction is modeled as a power low plus silicate features at 9.7 and 18 μm. The features are counted as a combination of measured galactic extinction profiles for these wavelengths (Smith et al. 2007).

2. IRS SPECTROSCOPY: OBSERVING STRATEGY AND REDUCTION

We have performed spectral mapping of the system NGC 4485/4490 by using the mapping mode of the IRS (Houck et al. 2004) on board *Spitzer*. Rectangular regions of 11.1 × 22.3 and 4.7 × 11.3 (i.e., zones of ∼0.42 × 0.84 and ∼0.18 × 0.42 kpc at the system) were mapped using both the Short-High (SH, ∼9.9–19.7 μm) and Long-High (LH, ∼19.5–38 μm) slits, respectively. Six rectangular regions centered at the positions of the ULXs (Table 1) were covered using a 1 × 4 and 1 × 7 grid array for the long and short slits of the IRS. In addition, two positions in NGC 4490 that are *not* near ULXs were observed with the same configuration as used for the ULXs. The integration time was 240 s at each position, and the step size is half the slit width perpendicular to the slit. This configuration allows net exposures of ≥480 s for rectangular sizes 16.7 × 22.3 and 14.1 × 11.3 for LH and SH slits, respectively.

Sets of eight exposures were taken for each position with the IRS. The prereduced Basic Calibrated Data (BCD) files were obtained from the *Spitzer* Science Center (SSC) database. In order to extract the spectra for the SH and LH modes, we used SMART (Spectroscopy Modeling Analysis and Reduction; Higdon et al. 2004), publicly available software provided by the SSC.[2]

3. INFRARED SPECTRAL DIAGNOSTICS

We have used line identifications from Smith et al. (2004), Armus et al. (2006), and NIST[3] (Martin et al. 1995). We combined both modes by rescaling the LH mode spectra to the SH mode spectra by adding or subtracting a constant and then rebinning to a resolution of 0.0287 μm pixel^{-1}. In Figure 1 we show the combined spectra from all the positions.

As we can see from Figure 1, some of the line features are

[2] Available at http://ssc.spitzer.caltech.edu/archanaly/contributed/smart/.

[3] Available at http://physics.nist.gov/PhysRefData/ASD/.

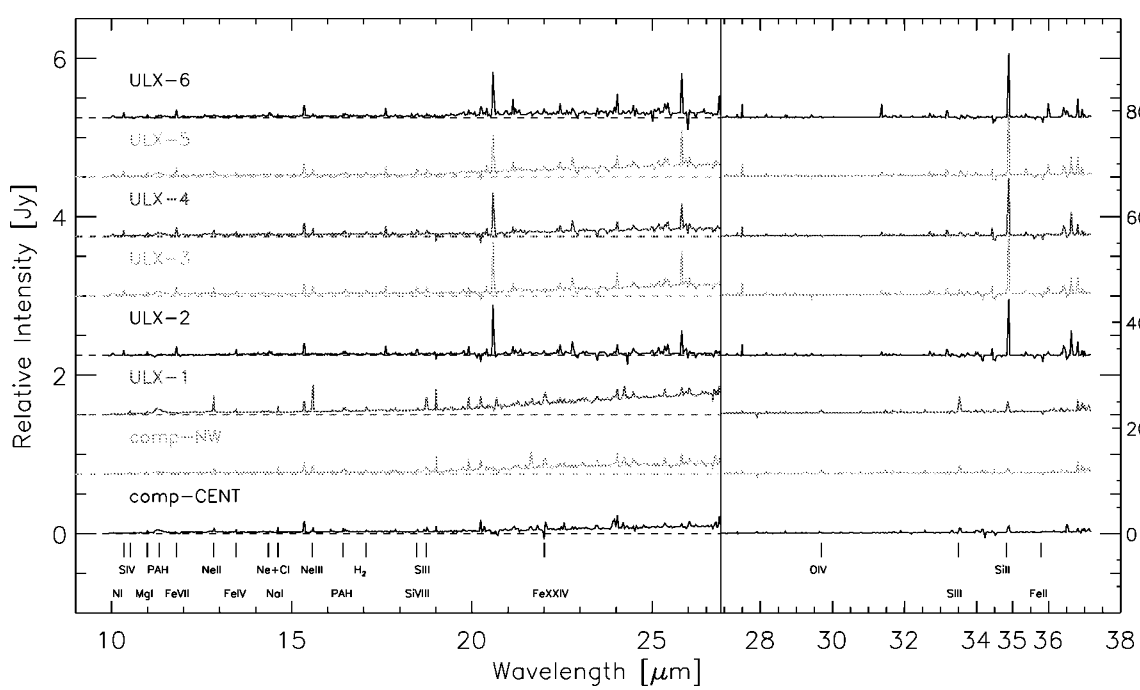

Fig. 1.—Combined spectra with the left SH and right LH modes for all of the sources analyzed in this study. For better visualization, the spectra have been plotted displaced along the *y*-axis. From ∼9 to ∼26.9 μm spectra are displaced by 0.75 Jy, and ∼26.9 to ∼38 μm spectra are displaced by 15 Jy. Dashed lines are set to help indicate the slope of the continuum at wavelengths ≥20 μm. [*See the electronic edition of the Journal for a color version of this figure*.]

only present or are stronger in the ULX region than in the comparison region spectra. The most striking examples are features such as [S IV] 10.51 μm, [Ne II] 12.81 μm, [Na I] 14.6 μm, [Ne III] 15.55 μm, [S III] 18.71 μm, and [S III] 33.48 μm, which seem to be significantly stronger in the comparison regions and ULX-1 (which is thought to be a supernova remnant [SNR] rather than an accreting binary) than in the rest of the sources. In contrast, the [Si II] 34.82 μm line is stronger in ULX-2 to ULX-6.

The purpose of this work is to generate some emission-line diagnostic diagrams similar to commonly used optical emission-line diagrams, which have proven useful in separating accretion-dominated sources from those dominated by stellar sources (e.g., Baldwin et al. 1981; Kauffmann et al. 2006 and references therein). A popular mid-infrared diagnostic first put forth in an *ISO* spectroscopic survey of ultraluminous infrared galaxies (ULIRGs) by Genzel et al. (1998) and later explored by Peeters et al. (2004) plots the emission line ratio [O IV] 25.91 μm/[Ne II] 12.81 μm versus the strength of a mid-infrared polycyclic aromatic hydrocarbon (PAH) features. These two lines, however, are relatively weak and difficult to detect in lower luminosity systems. Taking advantage of the strong low-ionization line emission of [Si II] 34.82 μm, Dale et al. (2006) suggested alternative diagrams to distinguish AGNs from star formation (SF) regions, such as [Ne III] 15.55 μm/[Ne II] 12.81 μm and [S III] 33.48 μm/[Si II] 34.82 μm. These ratios proved to be successful in separating accretion-powered from SF-powered regions in the SINGS galaxy sample.

We have calculated these ratios for our eight spectra, shown in Figure 2. We have also plotted the data from Dale et al. (2006), which include nuclear and extranuclear regions from SINGS, the SMC/LMC, and Galactic H II regions. Errors in the emission-line flux calculations are around 10%. The boundaries in Figure 2 are defined with the same curves as in Dale et al. (2006). As we can see from Figure 2, ULX-2, ULX-3, ULX-4, ULX-5, and ULX-6 are in zone I, where Seyfert and LINER galaxies are observed, while ULX-1, comp-NW, and comp-CENT are located in zone III, as star-forming systems. For ULX-2 and ULX-6 the line ratio [S III] 33.48 μm/[Si II] 34.82 μm is <0.01, which is extremely low compared to the extragalactic objects in Figure 2.

The SINGS group has recently developed models (`pahfit`; Smith et al. 2007) to characterize PAH features. The models include starlight continuum, featureless thermal dust continuum, pure rotational lines of H_2, fine-structure lines, dust emission features, and dust extinction. The starlight continuum is represented by a blackbody emission fixed at $T_\star = 5000$ K. Nine thermal dust continuum components are represented by blackbodies at fixed temperatures $T_m = 35$, 50, 75, 90, 110, 135, 200, 300, and 500 K. The program `pahfit` performs a fit through 200 iterations, each iteration determining a χ^2 value for all nine temperatures, until a minimum value for χ^2 is found. Dust temperatures are based on the shape of the continuum spectrum. We show the corresponding fits in Table 1; ULX-2 and ULX-6 have hotter components, but the relative intensity of those components is low for ULX-1.

The presence of a hotter dust component will flatten the spectra for our range of wavelengths. This effect is seen in Figure 1 for ULX-2 and ULX-6. The rest of the parameters modeled will be the subject of a forthcoming paper (G. A. Vázquez et al. 2007, in preparation).

Finally, we have found a strong linear anticorrelation between the observed log (L_X) and log([S III] 33.48 μm/[Si II] 34.82 μm). The regression and intercept coefficients are -0.21 ± 0.05 and 39.09 ± 0.6, respectively, with a rms $= 0.08$.

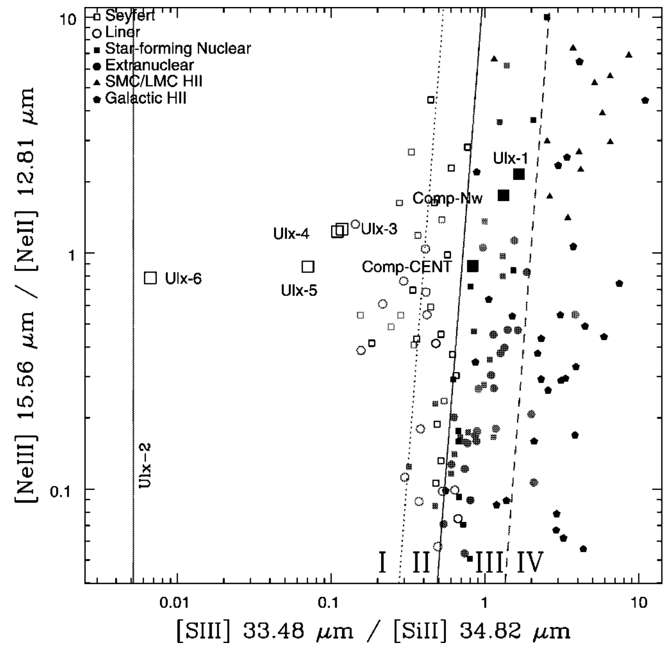

FIG. 2.—Neon, sulfur, and silicon diagnostic diagram showing line ratios for the eight regions in the NGC 4485/4490 system (names in black). Nuclear and extranuclear regions from the sample of SINGS (Dale et al. 2006) are also plotted, together with SMC, LMC, and Galactic H II regions. The vertical line for ULX-2 means that the value for the line ratio of [Ne III] 15.55 μm/[Ne II] 12.81 μm was not determined due to the undetected lines of Ne for this source. Zones III and IV are typical of SF regions. Objects in zones I and II can be classified as AGN-powered (Dale et al. 2006). [*See the electronic edition of the Journal for a color version of this figure.*]

4. DISCUSSION

For the first time, the IR continuum and lines (~9.9–38 μm) have been observed in ULXs using the power of the *Spitzer* IRS. It is likely that these ULXs are irradiating nearby star-forming clouds. Although the geometry is probably thus quite complex, we do find some hints of information as to the underlaying X-ray radiation. The most striking result from the data analyzed in this work is shown in Figure 2; five of the six ULXs reported by Roberts et al. (2002) fall in the "AGN zone" determined by the infrared diagnostic Ne, S, and Si emission line ratios (Dale et al. 2006). Both of the comparison regions used here, which do not harbor ULX sources, fall in the SF zone. The SF zone is also occupied by extranuclear star-forming regions in the SINGS galaxy sample and SMC/LMC and Galactic H II regions. The emission line at [N I] 10.33 and other unidentified features also behave like [Si II] 34.82 μm, showing a stronger contribution in ULX-2 to 6 than in ULX-1 or either of the comparison regions.

The presence of a hotter dust component in our PAH/continuum modeling (see Table 1) suggests that at least for ULX-2 and ULX-6 the [Si II] lines could be originating from an accreting source. A dilution factor could be affecting the rest of the ULXs, possibly due to their location within their host galaxy. All of this is consistent with the anticorrelation we have found between the line emission ratio of [S III] 33.48 μm/[Si II] 34.82 μm and the observed X-ray luminosity of the six ULXs; the more luminous the sources, the lower the ratio of these emission lines.

Different scenarios for the strong [Si II] line have been suggested in the literature. In these scenarios, the increasing density in H II, photodissociation (PDR), and X-ray dissociation regions (XDR), respectively, increases the intensity of the [Si II] 34.82 μm line (see Maloney et al. 1996; Kaufman et al.

2006; Meijerink & Spaans 2005). A third scenario suggests that heavy elements such as Si, Mg, and Fe may be returned to the gas phase by dust destruction (e.g., sputtering) in regions subject to strong shocks caused by stellar winds, starbursts, and AGN activity (Dale et al. 2006). Details of the geometry and ionization balance in the region require more detailed fitting, and also spatial mapping of spectral parameters, as ULXs are thought to have drifted from their birthplaces. The origin of these lines could thus be disentangled with detailed IRS mapping observations and IRAC imaging, which are the subject of a forthcoming paper (G. A. Vázquez et al. 2007, in preparation).

With the exception of a weak detection in ULX-1, we have not detected the emission line [O IV] 25.91 μm, a strong feature in SNRs (e.g., Morris et al. 2006; Williams et al. 2006), supporting previous suggestions that ULX-1 is a SNR (e.g., based on radio and X-ray constraints; Roberts et al. 2002).

The mid-infrared emission line diagnostics used to uncover the nature of AGNs and SF galaxies has been shown here to work well to separate SFRs and young supernovae from probable true accreting ULXs (according to X-ray observations; Roberts et al. 2002). But this is a small sample of ULXs to claim a general rule; it could be improved by observing a larger number of ULXs. The present work shows that a new diagnostic window has been opened on ULXs and their immediate environment via important mid-infrared features like [Si II] 34.82 μm, made observationally available by the extraordinary performance of the *Spitzer* IRS.

Many thanks to Danny A. Dale, who provided us his data for our figures. This work has been supported by the *Spitzer* grant 3360 (PI: E. Colbert).

REFERENCES

Armus, L., et al. 2006, ApJ, 640, 204
Baldwin, J. A., Phillips, M. M., & Terlevich, R. 1981, PASP, 93, 5
Colbert, E., & Mushotzky, R. 1999, ApJ, 519, 89
Colbert, E., & Ptak, A. 2002, ApJS, 143, 25
Colbert, E., et al. 2004, ApJ, 602, 231
Dale, D. A., et al. 2006, ApJ, 646, 161
Genzel, R., et al. 1998, ApJ, 498, 579
Higdon, S. J. U., et al. 2004, PASP, 116, 975
Hornschemeier, A. E., et al. 2004, ApJ, 600, L147
Houck, J. R., et al. 2004, ApJS, 154, 18
Kauffmann, G., Heckman, T. M., De Lucia, G., Brinchmann, J., Charlot, S., Tremonti, C., White, S. D. M., & Brinkmann, J. 2006, MNRAS, 367, 1394
Kaufman, M. J., Wolfire, M. G., & Hollenbach, D. J. 2006, ApJ, 644, 283
King, A. R. 2006, in Compact Stellar X-Ray Sources, ed. W. Lewin & M. van der Klis (Cambridge: Cambridge Univ. Press), 507
King, A. R., et al. 2001, ApJ, 552, L109
Laurent, O., et al. 2000, A&A, 359, 887
Lehmer, B. D., Brandt, W. N., Hornschemeier, A. E., Alexander, D. M., Bauer, F. E., Koekemoer, A. M., Schneider, D. P., & Steffen, A. T. 2006, AJ, 131, 2394
Liu, J.-F., & Bregman, J. N. 2005, ApJS, 157, 59
Maloney, P. R., Hollenbach, D. J., & Tielens, A. G. G. M. 1996, ApJ, 466, 561
Martin, W. C., Sugar, J., Musgrove, A., Dalton, G. R., Wiese, W. L., & Fuhr, J. R. 1995, NIST Database for Atomic Spectroscopy, Ver. 2.0, NIST Standard Reference Database 61 (Gaithersburg: NIST)
Meijerink, R., & Spaans, M. 2005, A&A, 436, 397
Miller, C. M., & Colbert, E. J. M. 2004, Int. J. Mod. Phys. D, 13(1), 1
Miller, J. M., Zezas, A., Fabbiano, G., & Schweizer, F. 2004, ApJ, 609, 728
Morris, P. W., et al. 2006, ApJ, 640, L179
Peeters, E., Spoon, H. W. W., & Tielens, A. G. G. M. 2004, ApJ, 613, 986
Ptak, A. F., & Colbert, E. J. M. 2004, ApJ, 606, 291
Ptak, A., & Griffiths, R. 1999, ApJ, 517, L85
Roberts, T., & Warwick, R. 2000, MNRAS, 315, 98
Roberts, T., et al. 2002, MNRAS, 337, 677
Smith, J. D. T., et al. 2004, ApJS, 154, 199
———. 2007, ApJ, 656, 770
Sturm, E., et al. 2002, A&A, 393, 821
Swartz, D. A., Ghosh, K. K., Tennant, A. F., & Wu, K. 2004, ApJS, 154, 519
Tully, R. B. 1988, Catalogue of Nearby Galaxies (Cambridge: Cambridge Univ. Press)
Williams, R. M., Chu, Y. H., & Gruendl, R. 2006, AJ, 132, 1877
Zezas, A., & Fabbiano, G. 2002, ApJ, 577, 726